The Target of β-Expansin EXPB1 in Maize Cell Walls from Binding and Solid-State NMR Studies[1][OPEN]

Tuo Wang[2], Yuning Chen[2], Akira Tabuchi, Daniel J. Cosgrove*, and Mei Hong*

Department of Chemistry, Massachusetts Institute of Technology, Cambridge, Massachusetts 02139 (T.W., M.H.); and Department of Biology, Pennsylvania State University, University Park, Pennsylvania 16802 (Y.C., A.T., D.J.C.)

ORCID IDs: 0000-0002-8730-6218 (Y.C.); 0000-0001-9012-3562 (A.T.); 0000-0002-4020-5786 (D.J.C.).

The wall-loosening actions of β-expansins are known primarily from studies of EXPB1 extracted from maize (*Zea mays*) pollen. EXPB1 selectively loosens cell walls (CWs) of grasses, but its specific binding target is unknown. We characterized EXPB1 binding to sequentially extracted maize CWs, finding that the protein primarily binds glucuronoarabinoxylan (GAX), the major matrix polysaccharide in grass CWs. This binding is strongly reduced by salts, indicating that it is predominantly electrostatic in nature. For direct molecular evidence of EXPB1 binding, we conducted solid-state nuclear magnetic resonance experiments using paramagnetic relaxation enhancement (PRE), which is sensitive to distances between unpaired electrons and nuclei. By mixing ^{13}C-enriched maize CWs with EXPB1 functionalized with a Mn^{2+} tag, we measured Mn^{2+}-induced PRE. Strong ^{1}H and ^{13}C PREs were observed for the carboxyls of GAX, followed by more moderate PREs for carboxyl groups in homogalacturonan and rhamnogalacturonan-I, indicating that EXPB1 preferentially binds GAX. In contrast, no PRE was observed for cellulose, indicating very weak interaction of EXPB1 with cellulose. Dynamics experiments show that EXPB1 changes GAX mobility in a complex manner: the rigid fraction of GAX became more rigid upon EXPB1 binding while the dynamic fraction became more mobile. Combining these data with previous results, we propose that EXPB1 loosens grass CWs by disrupting noncovalent junctions between highly substituted GAX and GAX of low substitution, which binds cellulose. This study provides molecular evidence of β-expansin's target in grass CWs and demonstrates a new strategy for investigating ligand binding for proteins that are difficult to express heterologously.

Expansins comprise the only group of plant proteins demonstrated to induce stress relaxation and long-term, irreversible extension (creep) of plant cell walls (CWs), which are essential for cell enlargement during plant growth (Cosgrove, 2000, 2016). Two major classes of plant expansins, α-expansins (EXPA) and β-expansins (EXPB), are recognized and both are present as multigene families in all land plants (Li et al., 2002; Sampedro and Cosgrove, 2005; Cosgrove, 2015). Expansin genes are also found in a variety of bacteria, fungi, and other microbes (Darley et al., 2003; Georgelis et al., 2014), acquired by horizontal gene transfer from plants (Nikolaidis et al., 2014). Analysis of BsEXLX1, the expansin from *Bacillus subtilis* (Kerff et al., 2008; Georgelis et al., 2015), has been particularly insightful for assessing the complex binding properties and functional targeting of this protein within the CW. Such progress was enabled by expression of BsEXLX1 in *Escherichia coli*, facilitating creation of site-directed mutants (Georgelis et al., 2011, 2012) and ^{13}C, ^{15}N labeling for solid-state NMR (SSNMR) analysis of EXLX1-CW interactions in muro (Wang et al., 2013). Compared with BsEXLX1, plant expansins have stronger wall-loosening activity and different selectivity, so their actions still require further study. Unfortunately, heterologous expression of active plant expansins has been difficult so far; thus, our understanding of their targets of action is based on limited studies with native proteins.

The CW-loosening activity of β-expansin is known primarily through studies of maize (*Zea mays*) EXPB1, which is abundantly expressed in pollen and is known in the immunology literature as *Zea* m 1d, a group 1 grass pollen allergen. Phylogenetic analysis shows that EXPB1 is part of a distinctive group of β-expansins that evolved uniquely in the grass family (Poaceae; Sampedro et al., 2015) and serve a biological function

[1] This research was financially supported by the Center for Lignocellulose Structure and Formation, an Energy Frontier Research Center funded by the U.S. Department of Energy, Office of Science, Basic Energy Sciences under award no. DE-SC0001090. EXPB1 preparation and binding experiments were supported by the U.S. Department of Energy Grant DE-FG02-84ER13179 to D.J.C. from the Office of Basic Energy Sciences. 900 MHz NMR spectra were measured at the MIT/Harvard Center for Magnetic Resonance, which is supported by NIH grant EB002026.

[2] These authors contributed equally to the article.

* Address correspondence to meihong@mit.edu and dcosgrove@psu.edu.

The author responsible for distribution of materials integral to the findings presented in this article in accordance with the policy described in the Instructions for Authors (www.plantphysiol.org) is: Daniel J. Cosgrove (dcosgrove@psu.edu).

T.W., Y.C., and A.T. performed the experiments; all authors contributed to the experimental design, data interpretation, and writing the manuscript; D.J.C. and M.H. conceived and supervised the project.

[OPEN] Articles can be viewed without a subscription.

www.plantphysiol.org/cgi/doi/10.1104/pp.16.01311

that appears to be unique among expansins, which is to facilitate penetration of the pollen tube through the stigma and style, thereby quickening delivery of sperm to the ovule (Valdivia et al., 2007, 2009). The crystal structure of EXPB1 was solved with native protein purified from maize pollen and shows two tightly packed domains forming an elongated ellipsoidal protein with a long, open, presumptive binding surface that spans the two domains (Yennawar et al., 2006).

EXPB1 induces stress relaxation and creep of CWs from grasses but has negligible loosening effect on dicot CWs (Cosgrove et al., 1997; Li et al., 2003; Sampedro et al., 2015). In contrast, α-expansin induces stress relaxation and creep of CWs from both dicots and grasses, in some cases with a greater effect on dicot CWs (McQueen-Mason et al., 1992; Cho and Kende, 1997; Sampedro et al., 2015). These observations led to the proposal (Li et al., 2003) that EXPB1 specifically targets glucuronoarabinoxylan (GAX), which is abundant in grass CWs but is largely absent in primary CWs of dicots (Carpita, 1996; Vogel, 2008).

Consistent with this idea, Tabuchi et al. (2011) found that treatment of maize CWs with EXPB1 induces release (solubilization) of a form of GAX with a high degree of arabinose substitution (hsGAX) as well as smaller amounts of homogalacturonan (HG). Extensive testing of EXPB1 did not detect any enzymatic activities, just as tests for enzymatic activities with α-expansins and bacterial expansins proved to be negative (McQueen-Mason and Cosgrove, 1995; Kerff et al., 2008; Georgelis et al., 2011, 2015). Moreover, EXPB1 caused marked mechanical weakening of grass CWs, as measured in tensile force/extension assays. These actions were likewise specific to grass CWs, as polysaccharide release and wall weakening were not seen when EXPB1 was applied to CWs from a variety of nongrass species, nor have they been found with α-expansins (McQueen-Mason and Cosgrove, 1995; Yuan et al., 2001; Tabuchi et al., 2011) or bacterial expansins (Georgelis et al., 2014). Thus, while EXPB1 action has commonalities with α-expansin action, namely induction of CW creep and stress relaxation, it also has unique features. The molecular details of these unique actions are not well understood, but they apparently entail structural features unique to grass CWs.

We set out in this study to assess EXPB1 binding with specific components of the grass CW. The primary CWs of grasses consist of cellulose (approximately 20–60%), GAX (approximately 20–35%), mixed-linkage glucan (MLG; approximately 5–20%, transient), xyloglucan (XyG, approximately 2–10%), and pectic polysaccharides (approximately 5–10%). The percentages shown here are based on analyses of maize and barley coleoptiles and vary by developmental stage (Carpita, 1996; Carpita et al., 2001; Gibeaut et al., 2005). The most notable differences between dicot and grass CW compositions are the low amount of pectins and XyG and the high content of GAX in grass CWs. GAX varies considerably in arabinose substitution, and this variation correlates with binding to cellulose (Carpita, 1983): hsGAX (Ara: Xyl $>$ 0.6) is weakly held in the CW and may be extracted with calcium chelators and even water, whereas GAX with low substitution (lsGAX, Ara: Xyl of $<$ 0.5) is tightly bound in the CW and requires strong extractants such as 1 to 4 M NaOH for solubilization. GAX may also be oxidatively cross-linked via ferulate esterified to arabinose (Carpita et al., 2001; Buanafina, 2009), but EXPB1 does not break such cross links (Tabuchi et al., 2011).

To assess EXPB1 binding to grass CW polymers, in this study we quantified EXPB1 binding to whole CWs and to sequentially extracted CWs in which more tightly bound matrix polysaccharides were progressively removed. This approach was used previously to assess the binding target of α-expansin in dicot walls (McQueen-Mason and Cosgrove, 1995). We also employed a SSNMR technique, paramagnetic relaxation enhancement (PRE; Solomon, 1955; Bertini et al., 2001), to determine which wall polysaccharides are the closest to EXPB1. Unpaired electrons in paramagnetic ions or organic radicals enhance nuclear-spin T2 and T1 relaxation in a distance-dependent fashion. The PRE effect is sensitive to electron-nuclear distances up to approximately 2 nm (Nadaud et al., 2009; Jaroniec, 2015), which is much longer than the distances measurable from nuclear-spin dipolar couplings. PRE solid-state NMR has been used to refine protein structure (Sengupta et al., 2012, 2015), measure the depth of insertion of membrane proteins in lipid bilayers (Buffy et al., 2003; Su et al., 2012; Marbella et al., 2013; Maltsev et al., 2014), and study metal ion complexation in bacterial CWs (Kern et al., 2010). Here we demonstrate a novel application of PRE NMR, where EXPB1 extracted from natural sources is functionalized with a paramagnetic EDTA-Mn^{2+} tag to allow the determination of the polysaccharide binding target, without the need for recombinant ^{13}C, ^{15}N-labeled protein.

Both binding assays and PRE SSNMR data indicate that EXPB1 binds primarily to GAX, while binding to cellulose is negligible. More specifically, the PRE SSNMR spectra show that the GlcA residues in GAX experience the strongest PRE by Mn^{2+}-tagged EXPB1, followed by carboxyl groups in pectins. These results represent the first molecular evidence to our knowledge of the β-expansin binding target in grass CWs and offer insights into the loosening mechanism of EXB1.

RESULTS

EXPB1 Binding to Maize CWs

CW binding to EXPB1 was first characterized by depletion isotherms carried out in 20 and 50 mM NaOAc, adjusted to pH 5.5, using CWs isolated from maize silks. We used these CWs because EXPB1 normally interacts with silks in nature (Valdivia et al., 2009). These buffers were chosen because they are commonly used to assay CW creep activity (Li et al., 2003). The isotherms (Fig. 1A) show saturable binding,

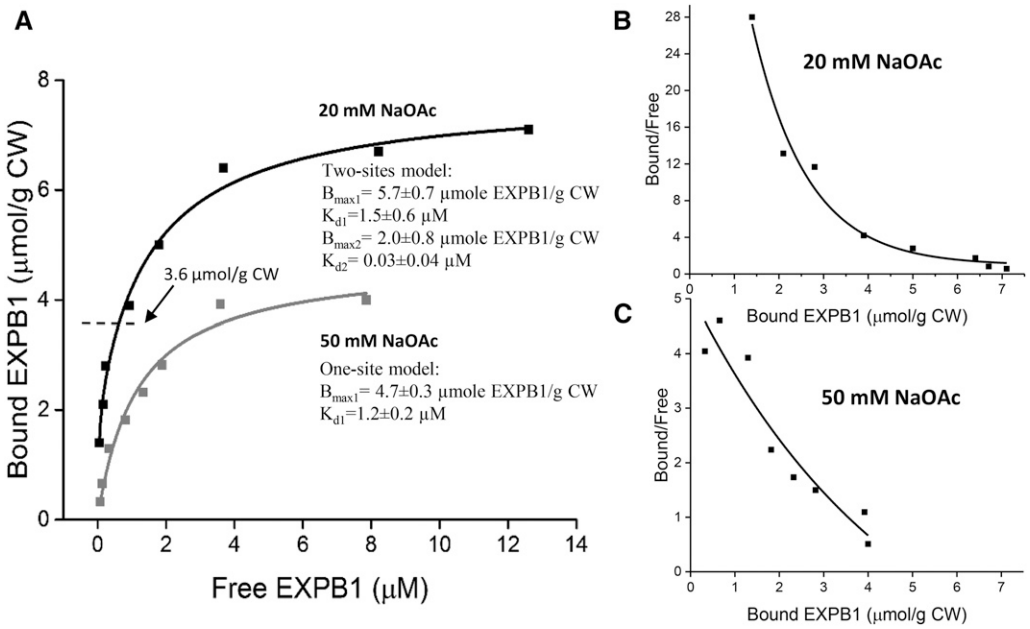

Figure 1. EXPB1 binding to maize CW in 20 mM and 50 mM NaOAc. A, Bound EXPB1 as a function of free EXPB1. The binding curves are best-fit to one-site and two-site Langmuir models for low and high concentrations of NaOAc. B and C, Scatchard plots of the binding data with trend lines, confirming the distinct binding patterns under the two conditions.

with approximately 60% greater binding in 20 mM NaOAc. Parallel measurements of CW extension (creep) show higher activity in 20 mM NaOAc than in 50 mM NaOAc (Supplemental Fig. S1). EXPB1 shows strong CW creep activity under conditions corresponding to approximately 1.5 μmol EXPB1 bound per gram CW, that is, at the initial (steep) part of these binding isotherms. The EXPB1-binding capacity of maize CWs thus greatly exceeds the amount of EXPB1 needed for robust CW creep activity.

EXPB1 binding in 50 mM NaOAc fits well to a single-site Langmuir model, whereas a two-site Langmuir model is a better fit for binding in 20 mM NaOAc solution (Fig. 1A). This difference in binding kinetics is also seen in Scatchard plots (Fig. 1, B and C), where a high-affinity binding site (K_d 0.03 μM) is observed in 20 mM NaOAc but not in 50 mM NaOAc. This result indicates that binding properties are sensitive to buffer strength or ionic conditions. Because of the complex nature of the CW, these fitting parameters are best viewed at this point as empirical summaries of binding characteristics without a more specific molecular interpretation.

Additional experiments showed that binding was largely insensitive to pH in the range of 4.0 to 5.5 (Supplemental Fig. S2) but was inhibited >90% by addition of various salts in a concentration-dependent manner (Fig. 2), indicating that EXPB1 binding to the CW is strongly electrostatic. At low added ionic strength (12 mM), Al^{3+} was appreciably more effective at inhibiting binding than Na^+, indicating a partial specificity of Al^{3+} interference with binding beyond simple ionic strength, but this difference was reduced at higher ionic strengths as binding was strongly inhibited (Fig. 2, inset). There was little difference in the effectiveness of Ca^{2+} and Mg^{2+} in inhibiting EXPB1 binding, indicating that the well-known specific interaction of Ca^{2+} with pectins does not affect EXPB1 binding. Together, these results suggest that EXPB1 binds preferentially to GAX, which is the predominant, weakly acidic polysaccharide in the maize CW (Carpita, 1996; Carpita et al., 2001).

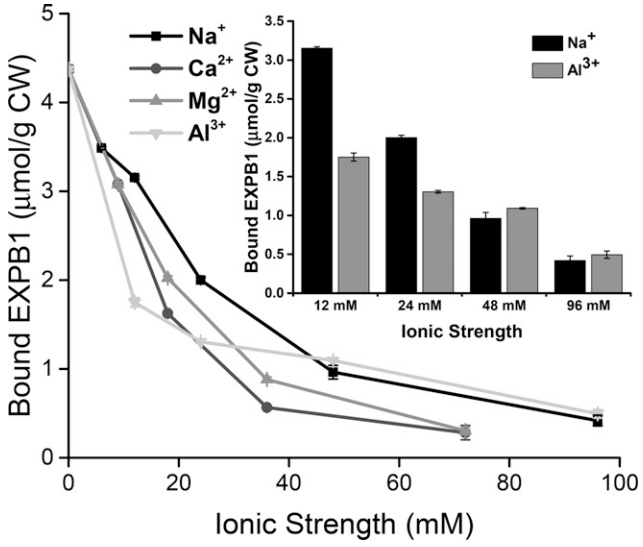

Figure 2. EXPB1 binding to maize silk CW in 20 mM NaOAc as a function of the ionic strength of added Cl^- salts. Inset compares Al^{3+} and Na^+ effects, showing larger attenuation of binding by Al^{3+} at low ionic strength. Total EXPB1 was 7.8 μmol/g CW. Means ± SE of 3 replicates.

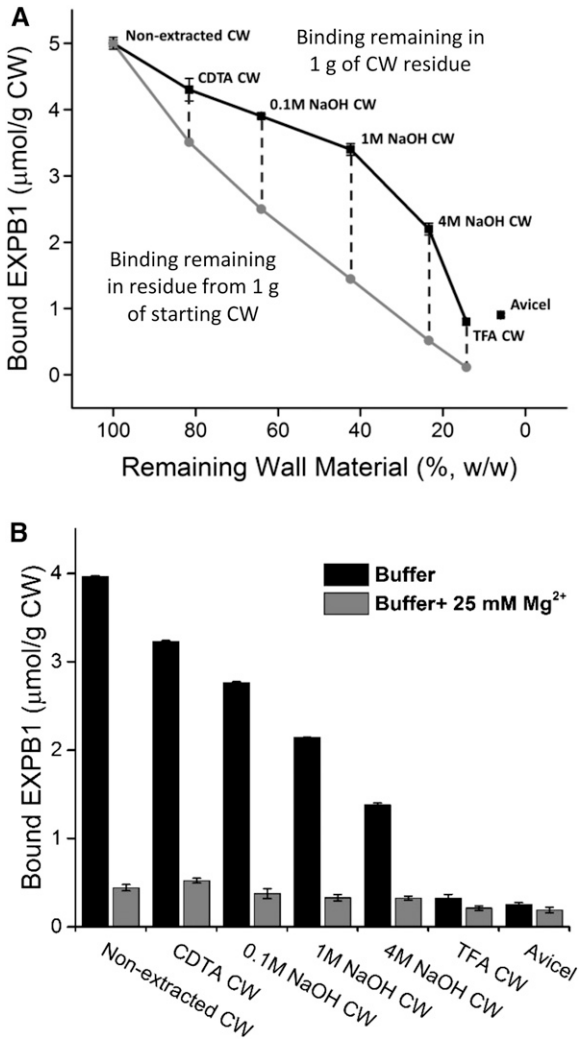

Figure 3. EXPB1 binding to sequentially extracted CWs. A, Amount of EXPB1 bound to extracted CW residues, expressed per gram CW residue (black, top curve) or per gram of starting material (gray, bottom curve). B, Reduction of EXPB1 binding by salt (25 mM $MgCl_2$) in the sequentially extracted CW samples. Assayed in 20 mM NaOAc with total EXPB1 of 7.8 μmol per gram CW in A and 6.1 μmol per gram CW in B. Means ± SE of three replicates.

To test this inference further, we assessed EXPB1 binding to CWs that were extracted sequentially to first remove weakly bound pectins and hsGAX, then more tightly bound lsGAX, MLG, and XyG. A final trifloroacetic acid (TFA) hydrolysis step removed noncrystalline polysaccharides, leaving crystalline cellulose as the residue. EXPB1 binding to the extracted residues decreased almost linearly in proportion to the loss of material from the CW, shown by the lower gray line in Figure 3A. When expressed per gram of CW residue (Fig. 3A, top line), the loss of EXPB1 binding is found to be the steepest in the later extraction steps after 4 M NaOH, which swells cellulose and extracts tightly bound hemicelluloses, and particularly after TFA hydrolysis of noncrystalline polysaccharides. Thus, we infer that EXPB1 targets both weakly bound and strongly bound matrix polysaccharides, but with a preference toward the latter. Expansin binding to the TFA-hydrolyzed residue is comparatively weak and similar to binding to the commercial cellulose Avicel (Fig. 3; Supplemental Fig. S3). As was the case with unextracted CW, EXPB1 binding to the extracted CW residues was strongly reduced by added salt (Fig. 3B), except for cellulose. Sugar analysis of the CW residues and extracts (Supplemental Table S1) confirms that the first step in the extraction series removes pectins (approximately 60%; predominantly HG and a small amount of rhamnogalacturonan I) and hsGAX (approximately 30%). Sugar composition of the second extract (0.1 M NaOH) is consistent with hsGAX, while the compositions of the 1 and 4 M NaOH extracts are consistent with a mixture of GAX, XyG, and MLG. The composition and extraction patterns for this CW resemble that of previous work on maize coleoptiles (Carpita, 1983; Carpita et al., 2001). These results indicate that EXPB1 binds to both highly substituted and lowly substituted GAX in the grass CW, although additional binding to XyG and MLG cannot be excluded. Despite the strong electrostatic component of EXPB1 binding to the whole CW, substantial binding to pectins is not indicated by these results, because while 60% of the pectin is removed in the first extraction step, the residue retained most of the EXPB1-binding ability.

To test the idea that CW binding is essential for EXPB1 activity, we assessed the effect of salt on EXPB1-induced CW creep and release of feruoylated GAX from maize CWs (Tabuchi et al., 2011). As shown in Figure 4, A and B, 10 mM $CaCl_2$ strongly inhibited EXPB1-induced creep activity and likewise inhibited release of sugars and 320-nm absorbance, corresponding to feruoylated GAX. It is possible that the calcium inhibition of CW creep was caused by mechanical stiffening of CW by cross-linking of nonesterified HG by calcium. However, 10 mM $CaCl_2$ did not reduce elastic or plastic compliances of the walls, as measured in stress/strain assays (Fig. 4C), excluding a purely mechanical basis for the calcium inhibition of EXPB1 activity. Therefore, we conclude that the salt-induced inhibition of EXPB1 activities results primarily from reduced EXPB1 interaction with the CW. This is also consistent with the reduced CW creep in 50 mM versus 20 mM buffer (Supplemental Fig. S1).

Paramagnetic Tagging of EXPB1

To provide structural evidence of the expansin binding target, we conducted SSNMR PRE experiments. For this purpose, we prepared EDTA-Mn^{+2}-tagged EXPB1 and mixed it with hydrated ^{13}C-labeled maize CWs at a mass ratio of 0.1, corresponding to the mid part of the binding curve in 20 mM NaOAc (approximately 3.6 μmol EXPB1 per gram CW; Fig. 1A). This

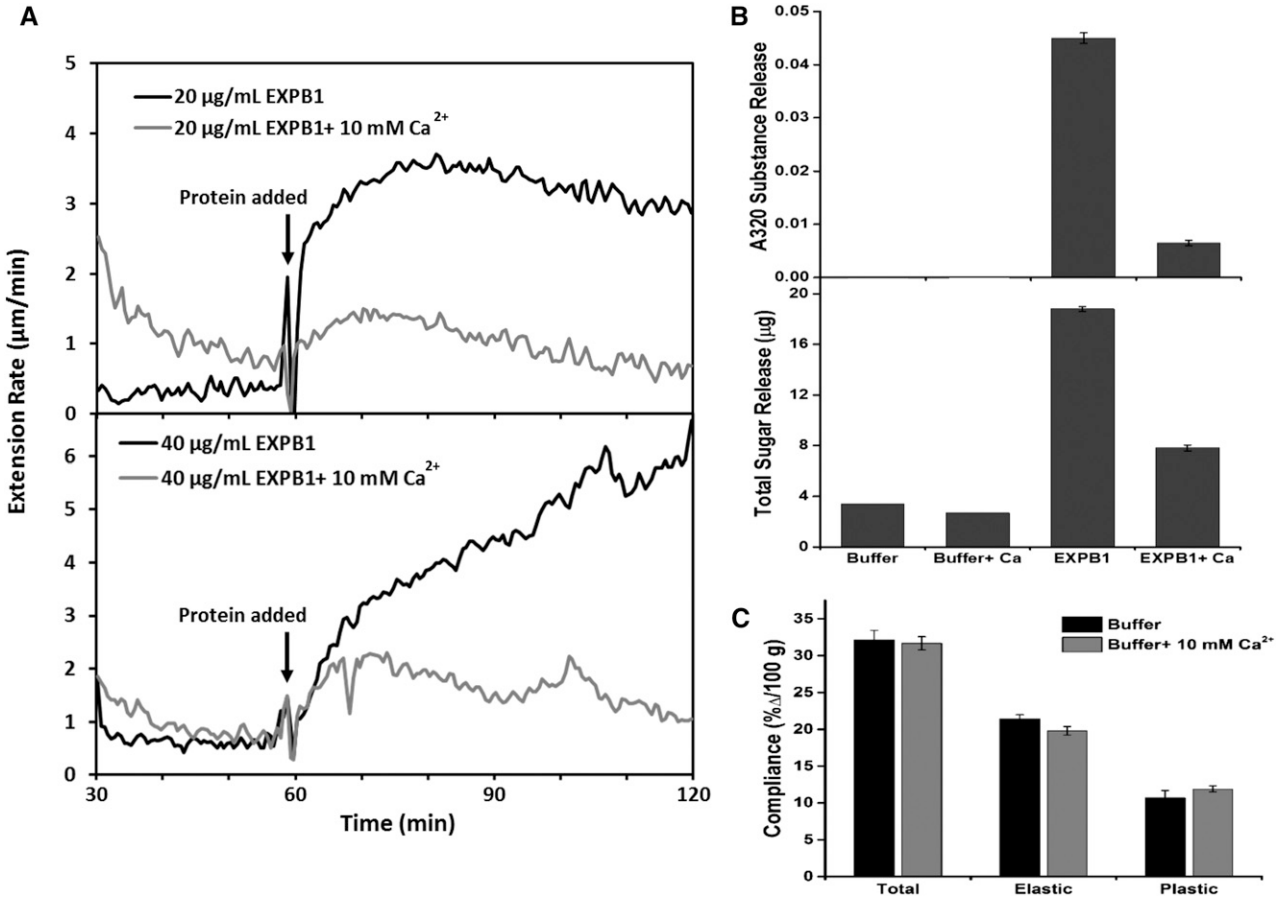

Figure 4. Inhibition of EXPB1 activities by 10 mM $CaCl_2$. A, Creep of wheat coleoptile walls upon addition of EXPB1 at two concentrations in the presence or absence of 10 mM Ca^{2+}. B, Release of feruoylated GAX (A320) and polysaccharide from 1 mg of maize silk CW after 20 h in 20 mM NaOAc with or without EXPB1 (100 µg/mL) and with or without 10 mM Ca^{2+}. C, Effect of Ca^{2+} on mechanical compliances of wheat coleoptile walls. In A, curves are means of 8 to 10 replicates; in B and C, the values are means ± 3 and 12 replicates, respectively.

concentration corresponds to the mid-high range of the activity-concentration curve for EXPB1 and is below its saturation point for wall extension activity (Li et al., 2003). The EDTA-Mn^{2+} tag was covalently attached to accessible free cysteines on the protein surface (Fig. 5). There are nine cysteines in EXPB1, six of which are involved in three conserved disulfide bonds (Yennawar et al., 2006), leaving three cysteines, C58, C128, and C156, accessible to solvent and potentially capable of binding EDTA-Mn^{2+}. C128 and C156 lie at the two ends of the protein, flanking the putative polysaccharide binding surface, while C58 is located at the bottom of a shallow cleft, close to the presumptive active site of EXPB1 domain 1. C58 is sterically less accessible than C128 and C156, so it may be less reactive with the EDTA tag. Electrospray ionization mass spectrometry (ESI-MS) analysis of the labeled protein showed that the dominant species incorporated two linkers/two Mn^{2+} ions (Supplemental Fig. S4A), while smaller signals were found for EXPB1 with two linkers/one Mn^{2+} and three linkers/three Mn^{2+}. Tagging did not alter EXPB1 binding to the CW (Supplemental Fig. S4B), but it partially inhibited CW creep activity (Supplemental Fig. S4D). The reduced activity may indicate partial steric hindrance of EXPB1 action by the EDTA-Mn^{+2} tags. Because tagging did not appreciably affect bulk binding characteristics, we expect the CW-EXPB1 interactions, as detected by SSNMR, to be similar to those of untagged EXPB1.

EXPB1 Targets Matrix Polysaccharides

Figure 6A compares quantitative ^{13}C direct polarization (DP) magic angle spinning (MAS) spectra of maize CWs with Mn^{2+}-tagged or untagged EXPB1. The spectra were measured with a long recycle delay of 25 s, so that the signals of dynamic and rigid polysaccharides are quantitatively represented. Most ^{13}C signals <110 ppm show similar intensities between the two samples, while the carbonyl region shows a clear intensity decrease for the 177-ppm peak in the paramagnetic sample. Spectral deconvolution indicates

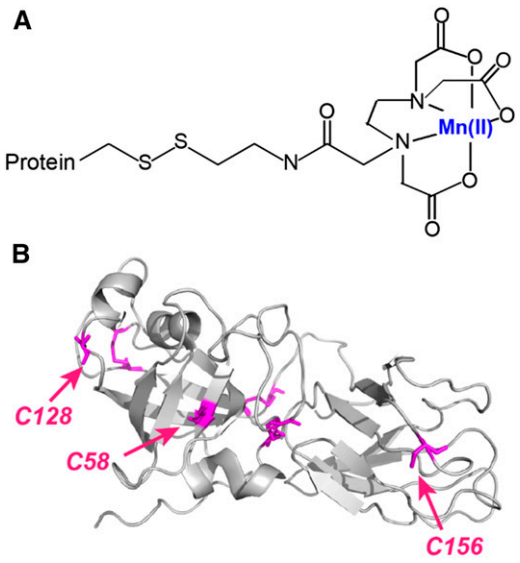

Figure 5. Mn^{2+} tagging of β-expansin. A, Modification of solvent-accessible Cys residues in proteins using [*S*-(2-pyridylthio) cysteaminyl] EDTA-metal (Ebright et al., 1992; Ermácora et al., 1992). B, The structure of EXPB1, *Zea* m 1 (PDB code 2HCZ), showing all nine Cys residues (magenta), among which are three solvent-accessible cysteines (red arrows) that can be modified with EDTA-Mn^{2+}. The other six cysteines form three disulfide bonds.

at least six peaks in this region (Fig. 6, B and C), four of which have narrow linewidths of 0.6 to 1.0 ppm. Based on previous resonance assignment of Arabidopsis (*Arabidopsis thaliana*) and *Brachypodium* CWs, we assign the 177-ppm peak to the carboxylate group in the GlcA residues of GAX (Wang et al., 2014), the 176-ppm peak to GalA in pectins, the 174-ppm peak to acetyl in RG-1 and GAX, and the 172-ppm peak to methyl esters in HG (Wang et al., 2012; White et al., 2014; Supplemental Fig. S5). Interestingly, this maize CW carbonyl spectral pattern resembles a composite of the spectra of the Arabidopsis and *Brachypodium* CWs: both share the GalA and acetyl peaks, but the Arabidopsis spectrum lacks the 177-ppm GlcA peak while the *Brachypodium* spectrum lacks the 172-ppm methyl ester peak. Thus, the maize CW contains significant amounts of both GAX and pectins. In addition to the well-resolved carbonyl peaks, two broad carbonyl peaks with full width at half maximum of approximately 7 ppm and approximately 2 ppm are necessary to fit the spectra (Supplemental Table S2). We tentatively assign these broad peaks to matrix polysaccharides that undergo segmental motions on the tens to hundreds of kilohertz timescale, which interfere with ^{1}H dipolar decoupling. Our previous correlation and relaxation experiments consistently found partial immobilization of some of the matrix polysaccharides, presumably due to binding to cellulose (Wang et al., 2012; Wang et al., 2014).

With the distinction of the multiple carbonyl peaks, we can see that the Mn^{2+}-tagged EXPB1 decreased the 177-ppm peak intensity to 57% of the intensity of the diamagnetic sample, with a concomitant increase of the peak line width from 135 Hz (0.6 ppm) to 225 Hz (1.0 ppm; Fig. 6, B and C). Thus, Mn^{2+}-tagged expansin preferentially enhances the T2 relaxation rate of GlcA in GAX. In contrast, the resolved

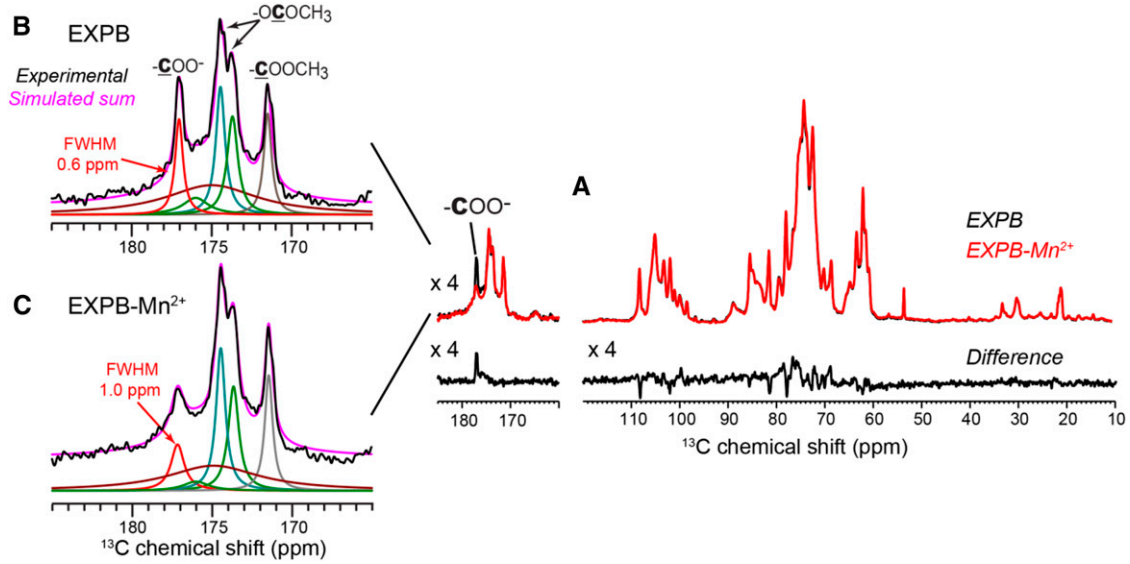

Figure 6. A, Quantitative ^{13}C DP spectra of maize CWs containing EXPB with (red) and without (black) Mn^{2+} tags. The spectra were measured at 296 K with a 25-s recycle delay. The difference spectrum shows that only carboxylate carbons are dephased by PRE, indicating protein binding. The small peak at 165 ppm is the spinning sideband of the 105-ppm peak. B, Spectral deconvolution of the carbonyl region of the EXPB control spectrum using Dmfit (Massiot et al., 2002). C, Spectral deconvolution of the carbonyl region of the EXPB-Mn^{2+} spectrum. Deconvolution indicates that the carboxylate linewidth increased from 0.6 ppm in the control sample to 1.0 ppm in the Mn^{2+} tagged sample, consistent with the PRE effect.

carbonyl peaks of pectins do not show intensity dephasing, indicating that expansin is further from pectins.

Although these quantitative ^{13}C DP spectra reflect the relative concentrations of dynamic and rigid polysaccharides, direct excitation of the ^{13}C magnetization has the disadvantage that PRE occurs on ^{13}C spins, whose low gyromagnetic ratio reduces the upper-limit distance that is measurable. The transverse PRE, $\Gamma \equiv R_2^{para} - R_2^{dia}$, depends on the electron-nuclear distance r and the nuclear-spin gyromagnetic ratio γ_n according to the Solomon-Bloembergen equation (Solomon, 1955; Bloembergen, 1957):

$$\Gamma_2 \approx \left(\frac{1}{15}\right)\left(\frac{\mu_0}{4\pi}\right)^2 \frac{\gamma_n^2 g_e^2 \mu_B S(S+1)}{r^6} \times \left(4T_{1e} + \frac{3T_{1e}}{1+\omega_n^2 T_{1e}^2} + \frac{13T_{1e}}{1+\omega_e^2 T_{1e}^2}\right),$$

where μ_0 is the vacuum permeability, g_e is the electron g-factor, μ_B is the Bohr magneton, S is the electron-spin

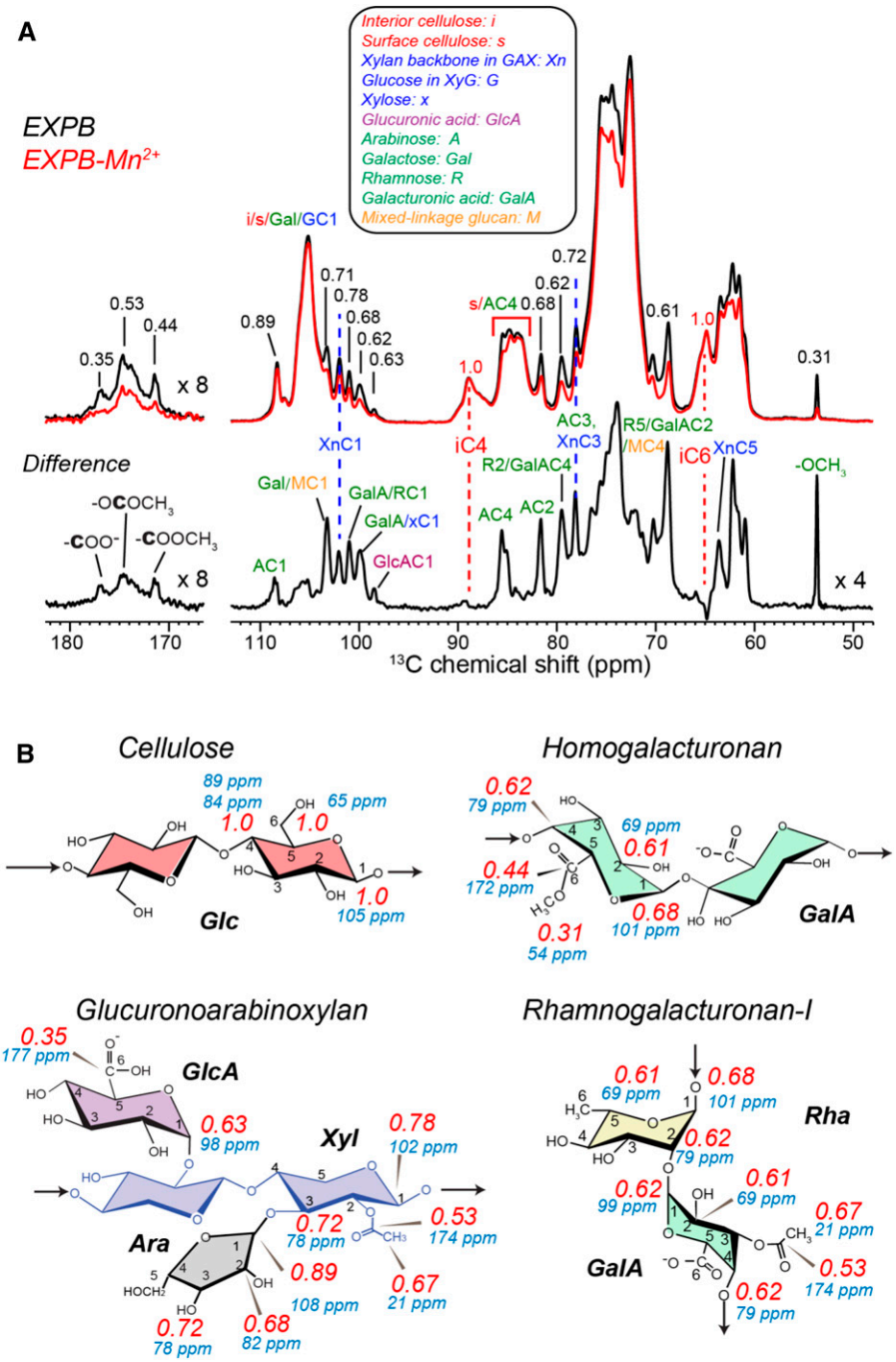

Figure 7. A, ^{13}C CP spectra of the EXPB1-containing maize CWs with (red) and without (black) Mn^{2+}. The difference spectrum shows only intensities of matrix polysaccharides, indicating that EXPB1 binds matrix polysaccharides but not cellulose. Assignment abbreviations used in this work are given. B, Intensity ratios (red) of the Mn^{2+}-containing spectrum and the control spectrum. The chemical shifts of the carbons are shown in blue. Cellulose does not show intensity decrease, indicating that it is far from EXPB1. GAX shows moderately low intensity ratios (0.7–0.9) for Xyl and Ara but much lower intensity ratios for GlcA carboxylate (0.35). Pectins also exhibit low intensity ratios of 0.3 to 0.7.

quantum number, and ω_n and ω_e denote the nuclear and electron Larmor frequencies, respectively. This equation indicates that the PRE scales with the square of the nuclear-spin gyromagnetic ratio; thus, for the same distances, the ^{1}H PRE should be 16-fold stronger than ^{13}C PRE, or conversely, the same ^{1}H PRE corresponds to 2.5-fold longer distances than ^{13}C PRE. To obtain longer distances, we measured the ^{13}C cross-polarization (CP) spectra (Fig. 7A), where the magnetization originates from ^{1}H spins. Indeed, Figure 7A shows significant intensity dephasing for many peaks in the paramagnetic sample, consistent with the detection of ^{1}H PRE due to Mn^{2+}. Interestingly, the difference spectrum between the two samples shows only sharp GAX and pectin signals while lacking cellulose signals, indicating that EXPB1 preferentially binds matrix polysaccharides. More quantitatively, Figure 7B summarizes the peak height ratios (S/S_0) between the EXPB1-Mn^{2+}-bound CW and the diamagnetic EXPB1-bound CW. These S/S_0 ratios depend on the average electron-nuclei distances, which take into account potential structural heterogeneities that may cause only a subpopulation of a polysaccharide in the CW to be close to expansin. Cellulose retains full signals in the presence of Mn^{2+}, indicating that it is uniformly far from EXPB1, while GAX and pectins show considerable dephasing, with S/S_0 ratios ranging from 0.31 to 0.89. Consistent with the ^{13}C DP spectra, the CP spectra show the lowest S/S_0 value at GlcA in GAX, indicating that EXPB1 binds GAX most strongly. However, the 54-ppm methyl ester carbon shows a similarly low S/S_0 value of 0.31, indicating that GalA in HG is strongly influenced by Mn^{2+}. Since this peak did not show detectable PRE in the ^{13}C DP spectra (Fig. 6), we conclude that EXPB1 preferentially binds the more rigid fraction of HG, while the mobile pectins, which dominate the quantitative DP spectra, are far from EXPB1.

The larger intensity decrease of the ^{13}C CP spectra compared to the DP spectra may not only result from stronger ^{1}H PRE than ^{13}C PRE but may also be influenced by preferential detection of rigid polysaccharides in the CP spectra. In these hydrated CW samples, the mass ratio of EXPB1 to total polysaccharide is about 1:10. Excluding the approximately 25 wt% of cellulose in the CW (Supplemental Table S1), the protein to matrix polysaccharide dry mass ratio is approximately 1:7.5. The ^{13}C CP experiments detect approximately 40% of the matrix polysaccharide signals, thus the CP-detected average protein to matrix polysaccharide mass ratio is approximately 1:3. This relatively high protein concentration makes it possible to detect significant intensity dephasing due to Mn^{2+} PRE.

To further resolve the ^{13}C signals that are indicative of site-specific Mn^{2+} PRE, we measured 2D PDSD spectra of the paramagnetic and diamagnetic samples (Fig. 8A). Upon first inspection, the two 2D spectra appear very similar, both dominated by cellulose signals. However, the difference 2D spectrum reveals clear intensity changes only of GAX and pectin peaks (Fig. 8, B and C), while the cellulose peaks show no intensity difference. The 2D spectra also resolved the surface cellulose signals from matrix-polysaccharide signals, for example in the 82- to 86-ppm region, where both arabinose and surface cellulose C4 peaks resonate, and in the 61- to 63-ppm region, where the surface cellulose C6 signal overlaps with the Gal C6, Xn C5, and Ara C5 signals. The improved spectral resolution reveals that the surface cellulose signals such as C4-C1

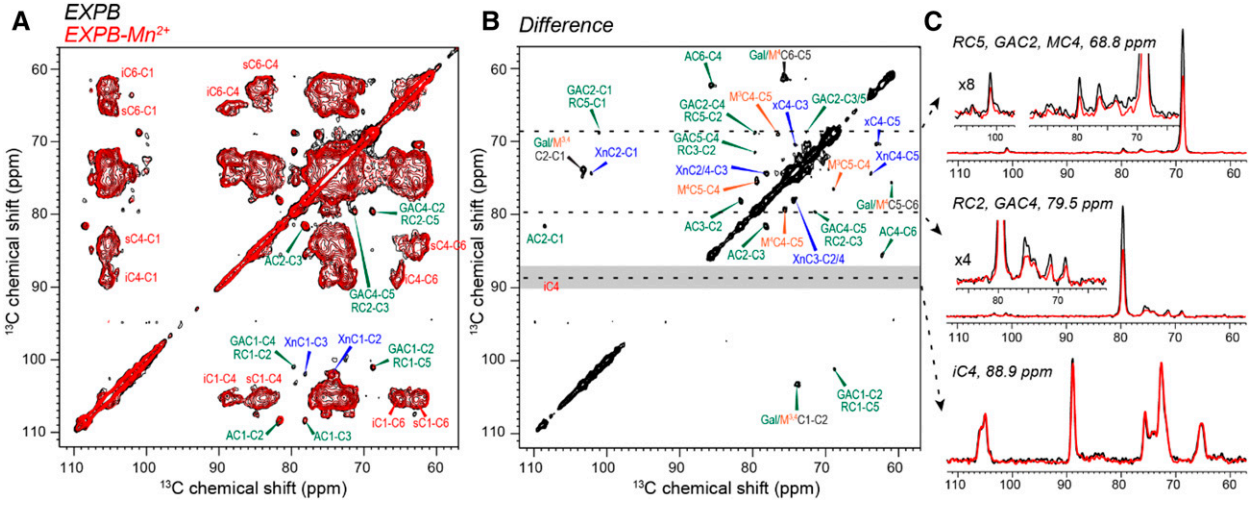

Figure 8. 2D ^{13}C-^{13}C CP-PDSD spectra of EXPB1-containing maize CWs. A, The 100-ms spectra of CWs with EXPB1 (black) and with Mn^{2+}-tagged EXPB1 (red). B, Difference spectrum, showing only matrix polysaccharide signals. Gray horizontal bar indicates the interior cellulose C4 position. C, Representative cross-sections of the 2D PDSD spectra. The diamagnetic (black) and paramagnetic (red) samples show identical cross-sections for cellulose, but the GAX and pectin signals are lower in the paramagnetic sample. Assignment abbreviations are given in Figure 7.

at (85, 105) ppm and C6-C4 at (62, 85) ppm are absent in the difference spectrum, further confirming that EXPB1 is far from cellulose, including the microfibril surface.

EXPB1 Changes GAX Mobility

To investigate the effect of EXPB1 on polysaccharide mobility, we measured ^{13}C-^{1}H dipolar couplings and C-H order parameters (S_{CH}) with and without EXPB1. The DIPSHIFT experiment detects the amplitudes of motion of C-H bonds on the submicrosecond timescale. The protein-containing CWs show very similar order parameters as protein-free CWs in the quantitative ^{13}C DIPSHIFT experiment (Fig. 9), indicating that the average motional amplitudes of the two samples are the same. However, in the CP-DIPSHIFT experiment, which preferentially detects more rigid molecules, the GAX signals show larger dipolar couplings or order parameters, indicating that the motional amplitudes decrease in the presence of the protein, while cellulose and pectin motions are not affected by protein binding (Fig. 9; Supplemental Fig. S6). Thus, the more rigid portion of GAX is further immobilized by EXPB1, whereas the more mobile portion of GAX increases the motional amplitudes so that the average GAX signals show no net change ± EXPB1.

DISCUSSION

The binding isotherms and SSNMR data presented here indicate that the main target of EXPB1 binding in maize CWs is GAX. This conclusion is supported by binding studies with sequentially extracted CWs, by inhibition of EXPB1 binding by salts, and by preferential PRE to GlcA residues of GAX. This conclusion is also consistent with the selectivity of EXPB1 action: EXPB1 loosens GAX-containing grass primary CWs but has little effect on dicot CWs, which are rich in GalA-containing pectins but lack GAX (Li et al., 2003; Sampedro et al., 2015; Carpita, 1996). Moreover, the PRE NMR data (Fig. 7) show that EXPB1 does not bind cellulose in whole CW mixtures, even though it binds isolated cellulose in vitro (Supplemental Fig. S3).

EXPB1 binding to GlcA is most likely electrostatic. The protein contains 31 cationic residues (22 Lys and 9 Arg) but only 22 anionic residues (13 Asp and 9 Glu),

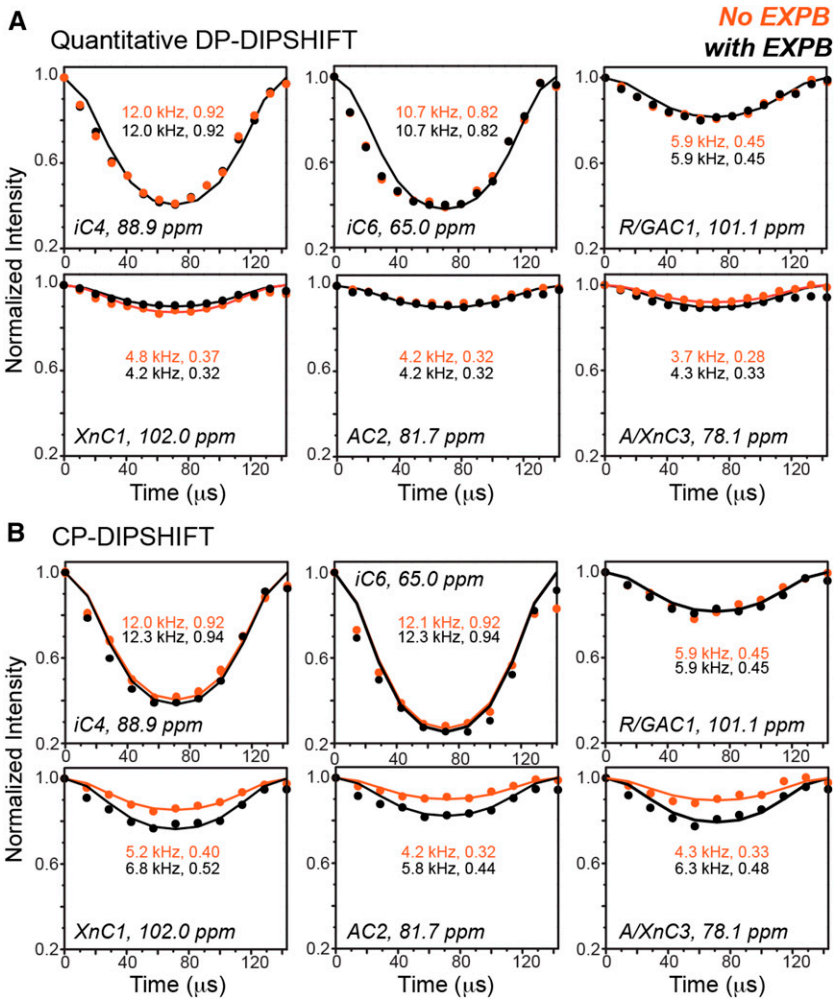

Figure 9. ^{13}C-^{1}H DIPSHIFT dipolar curves of maize CWs measured with quantitative ^{13}C DP (A) and ^{1}H-^{13}C CP (B). All spectra were measured at 296 K under 7 kHz MAS. The best-fit ^{13}C-^{1}H dipolar couplings and dipolar order parameters are indicated for each panel. CWs without and with EXPB1 are plotted in orange and black, respectively. The DP-DIPSFHIT data were measured using a long recycle delay of 20 s and detect all the molecules in a quantitative manner, while CP-DIPSHIFT preferentially detects the signals of rigid polysaccharides.

has a pI of 9.5 (Li et al., 2003), and all cationic residues are located on the protein surface. Thus, in 20 mM NaOAc at pH 5.5, the protein is positively charged, favoring electrostatic interactions with the negatively charged GlcA and GalA residues in matrix polysaccharides.

^{13}C-^{1}H dipolar order parameters indicate that EXPB1 exerts a complex effect on GAX mobility: the rigid portion of GAX became more rigid upon protein binding while the mobile portion became more dynamic. In contrast, cellulose and pectin mobilities were unaffected by the protein: cellulose retained the same near rigid-limit couplings, while pectins exhibited the same low-order parameters. Thus, although PRE of pectins was observed in the ^{13}C CP spectra, EXPB1 did not change the mobilities of pectins, while EXPB1 immobilized some of the GAX. Combined with the fact that the quantitative ^{13}C DP spectra exhibit only ^{13}C PRE to GAX, these data indicate that EXPB1 binds GlcA-rich arabinoxylan more strongly than GalA-rich pectins in grass CWs. Since both GAX and pectins contain negatively charged carboxyl groups, we attribute this difference in EXPB1 affinities to conformational differences between GAX and pectins. EXPB1 has a long, shallow groove formed by highly conserved polar and aromatic residues. This groove is about 47 Å long, spans both EXPB1 domains, and could accommodate a GAX backbone of up to 10 sugar residues (Yennawar et al., 2006). This shallow and relatively flat groove is less likely to fit the helical conformation of HG or the highly branched RG-1. The GAX-EXPB1 binding may be further stabilized by specific interactions between GAX and polar and aromatic residues on the protein surface (Yennawar et al., 2006; Sampedro et al., 2015). Attempts to crystallize a complex of EXPB1 and GAX have so far not been successful (Y. Chen, N. Yennawar, D.J. Cosgrove, unpublished data), so other means to test this hypothesis are needed.

A Model of EXPB1-Mediated CW Loosening

Our results indicate that EXPB1 has negligible interaction with cellulose but binds GAX and changes its mobility, potentially by unlocking GAX-GAX junctions in grass CWs. This new information complements previous data showing that EXPB1 specifically loosens grass CWs and solubilizes hsGAX from maize CWs (Li et al., 2003; Tabuchi et al., 2011). Previous biochemical data indicate that hsGAX displays only weak binding to cellulose (Carpita, 1983), thus it is unlikely to serve as a load-bearing linker directly interconnecting cellulose microfibrils but may act as space-filling interstitial material between cellulose microfibrils (Carpita et al., 2001). Additionally, it could serve a load-bearing role if it bound to matrix polysaccharides that in turn bind tightly to cellulose. Candidate polysaccharides that bind tightly to cellulose include lsGAX, XyG, and MLG (Carpita et al., 2001). We focus on lsGAX because our new data indicate the rigid component of GAX, which is presumably lsGAX, becomes more rigid after EXPB1 treatment. Figure 10 sketches a potential mechanism by which EXPB1 may exert its loosening effects on grass CWs. In this scheme, hsGAX binds to lsGAX, thereby indirectly spanning multiple cellulose microfibrils; we propose that EXPB1 may bind and disrupt the hsGAX-lsGAX junctions. Consistent with this scenario, lsGAX is known to bind to cellulose in vitro (Carpita, 1983; Köhnke et al., 2011; Selig et al., 2015), whereas hsGAX does not. Strong GAX-cellulose cross peaks are seen in 2D SSNMR spectra of *Brachypodium*, a model grass species, indicating subnanometer contacts between the two polysaccharides (Wang et al., 2014), which is also supported by the presence of a cellulose form that is restructured by interactions with GAX in *Brachypodium* and XyG in Arabidopsis CWs (Wang and Hong, 2016; Wang et al., 2016). If EXPB1 selectively disrupted noncovalent junctions between hsGAX and lsGAX, as envisioned in Figure 10, it would result in (1) increased mobility and solubilization of hsGAX, (2) decreased mobility of lsGAX, which would now interact more strongly with cellulose, and (3) promotion of CW stress relaxation and extension as a result of removal of the load-bearing hsGAX. These are the known actions of EXPB1 on grass CWs. In this scheme, release of HG would be incidental to solubilization of hsGAX. For EXPB1 acting on grass CWs, these actions would also weaken the middle lamella, which in grasses is composed of GAX and HG (Ishii, 1984), thereby promoting pollen tube penetration between cells of the maize stigma and style (Valdivia et al., 2007, 2009). This model may apply specifically to the clade of β-expansins that include group-1 grass pollen allergens, but additional work is needed to test its applicability to other groups of β-expansins and to other types of GAX-containing CWs (Sampedro et al., 2015).

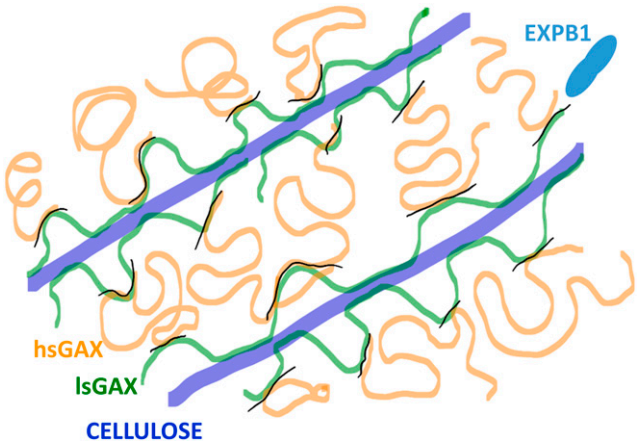

Figure 10. Conceptual scheme to account for the known CW-loosening and -binding activities of maize EXPB1. In this limited depiction of the grass CW, lsGAX binds to cellulose surfaces and hsGAX binds to lsGAX but not cellulose. EXPB1 is hypothesized to disrupt the noncovalent junctions (depicted as short black lines) between hsGAX and lsGAX. The result is solubilization of hsGAX and physical weakening of the grass CW.

Helical Conformation of Xylan Backbone of GAX from C4 Chemical Shifts

The ^{13}C chemical shifts of GAX in maize CWs are very similar to those in *Brachypodium* (Wang et al., 2014). The XnC4 chemical shift is sensitive to conformational changes of glycosidic bonds (Viëtor et al., 2002) and has been used as an indicator of the helical conformation of xylan in a recent SSNMR study (Dupree et al., 2015). MD simulation suggests that xylan in solution adopts a 3-fold helical screw (3_1-fold, three residues per 360° twist) but is folded as a 2-fold helical screw (2_1-fold, two residues per 360° twist) once adsorbed onto cellulose surface. The latter should better align with the 2_1 conformations of glucan chains (Bromley et al., 2013; Busse-Wicher et al., 2014). The typical XnC4 chemical shift is 76 to 78 ppm in solution (Vignon and Gey, 1998; Hollmann et al., 2009; Busse-Wicher et al., 2014) but changes to 79 to 85 ppm in the dry secondary CW of Arabidopsis, indicating a broad distribution of conformations with only a minor population adopting the 3_1-fold conformation (Dupree et al., 2015). In comparison, in the current maize CW samples, the XnC4 chemical shift is 74 ppm, which is similar to the chemical shifts in solution but different from the chemical shifts of xylan in Arabidopsis secondary CW (Dupree et al., 2015). Thus, the GAX backbone in maize primary CW may adopt a conformation similar to the 3-fold helical conformation in solution, implying that much of the GAX is well solvated and not tightly adsorbed onto cellulose surfaces. Future chemical shift calculations may be useful for correlating the NMR chemical shifts with the detailed conformations of xylan in different CWs (Kubicki et al., 2013, 2014; Watts et al., 2013; Zhao et al., 2014).

MATERIALS AND METHODS

EXPB1 Purification

Maize (*Zea mays*) pollen was collected in July 2014 at Rock Springs Farm (University Park, PA). EXPB1 was eluted from pollen with 50 mM NaOAc (adjusted to pH 4.5 with glacial acetic acid) containing 100 mM NaCl and fractionated stepwise by cation ion-exchange CM Sepharose (Sigma-Aldrich no. CCF-100) and ENrich (Bio-Rad no. 780-0021) chromatography and further fractionated on a Discover C5 reverse-phase HPLC column (Sigma-Aldrich no. 568422) (Li et al., 2003; Tabuchi et al., 2011).

Silk CW Preparation, Extraction, and Binding

Frozen maize silks (approximately 50 g wet weight) were ground to a fine powder by ball milling, washed sequentially with 1.5% (w/v) SDS and water, and then resuspended in 50 mL 50 mM HEPES buffer, pH 6.8, containing 20 units porcine amylase (Sigma-Aldrich no. A3176) to remove starch and 2 mM NaN_3 to inhibit microbial growth. CWs were digested for 20 h at 37°C with constant stirring, then rinsed in water and lyophilized. For some experiments, we sequentially extracted silk CWs (with 50 mM cyclohexane diamine tetraacetic acid, 0.1 M NaOH, 1 M NaOH, and 4 M NaOH) as described (Tabuchi et al., 2011). The residue after 4 M NaOH extraction was hydrolyzed with 2 M TFA at 121°C for 2 h. Wall residues at each step were washed 5× with water before dialysis against water for 48 h to remove salts. The extracted polysaccharides were desalted by membrane filters (3-kD molecular weight cutoff) and lyophilized. Wall/polysaccharide constituents were analyzed by monosaccharide analysis using ion chromatography (Dionex ICS5000 with Carbopac column and pulsed amperometric detection), as described previously (Tabuchi et al., 2011). Various amounts of EXPB1 were bound to 1 mg CW residues in 20 mM NaOAc buffer, pH 5.5, to a total volume of 400 μL. Binding equilibrium was established by shaking at 1,100 rpm for 1 h at 26°C. Residual EXPB1 in the supernatant was determined by Bradford protein assay kit (Thermo). Binding isotherms and Langmuir fits were analyzed with Origin v9.1 curve-fitting software (Microcal).

EXPB1 Function ± Ca^{2+}

Phenolics/Polysaccharide Release

A total of 1 mg nonextracted silk CW was incubated with 100 μg/mL EXPB1 in 500 μL 20 mM NaOAc buffer, pH 5.5, with 5 mM DTT to maintain expansin activity and 2 mM NaN_3 to retard microbial growth, and shaken at 1,000 rpm for 20 h ± 10 mM $CaCl_2$. Release of feruoylated GAX into the supernatant was assayed by 320-nm absorbance and the released sugar was measured with the phenol-sulfuric acid method (Dubois et al., 1956).

Mechanical Compliances

Four-day-old etiolated wheat coleoptiles were abraded, heat-inactivated, and incubated in 20 mM NaOAc buffer, pH 5.5, ±10 mM $CaCl_2$ for 30 min and extended twice at 3 mm/min to a target force of 10*g*. The total, elastic, and plastic compliances were calculated from the slopes of the force/extension curves as detailed by Cosgrove (2011).

Wall Extension (Creep)

Coleoptile walls were prepared as above, clamped into a constant force extensometer at 20*g* force, and incubated in 20 mM NaOAc buffer, pH 5.5, containing 2 mM DTT for 30 min to establish a stable baseline. The buffer was replaced with same buffer ±10 mM $CaCl_2$. The specimens were incubated for another 30 min before the addition of EXPB1.

Mn^{2+} Labeling of EXPB1

Linker (thiol-specific disulfide reagent, *N*-[*S*-(2-pyridylthio)cysteaminyl] EDTA; Toronto Research Chemicals) was dissolved in 50 mM NaOAc buffer (pH 5.5, filtered through a 0.45-μm syringe filter) to a concentration of 5 mg/mL and 100 μL linker solution (1 μmol) was mixed with 1 μL of 1 M $MnCl_2$ (99.999%; Sigma-Aldrich) in deionized water and incubated at 4°C for 2 h to load Mn^{2+} onto the EDTA. EXPB1 was purified by reverse-phase HPLC, and 2.8 mg (0.1 μmol) was mixed with linker-Mn^{2+} solution. The reaction volume was brought to 200 μL by adding 50 mM NaOAc buffer, pH 5.5, and allowed to react overnight at 4°C. Excess linker-Mn^{2+} was removed by filtration through a 3-kD cutoff membrane. Incorporation of linker-Mn^{2+} was assessed by ESI-MS (Proteomics and Mass Spectrometry Core Facility, PSU), and creep activity of labeled EXPB1 was assayed by extensometer assay.

^{13}C Uniform Labeling of Maize CWs

Maize seeds were surface sterilized twice (5 min/sterilization) in 50% bleach with 0.05% (v/v) Tween 20 and soaked overnight in sterile water. Endosperms were removed manually and the embryos were cultured in Murashige and Skoog medium (4.3 g MS salts [Sigma-Aldrich], 0.55 g MES·H_2O per liter, adjusted to pH 5.7) containing 5 g/L ^{13}C-Glc for 4 d in the dark at 27°C with 130 rpm shaking. Coleoptiles were collected, frozen in liquid nitrogen, and ground to a fine powder with a mortar and a pestle. CWs were prepared as described above for maize silks. Amylase-digested walls were washed with water, then centrifuged at 1,000*g* for 5 min and 5,000*g* for 60 min with a 40-μm nylon membrane filter to reduce water content to approximately 75%. A wet mass of 50 mg, which is estimated to contain approximately 12 mg dry mass, was used to bind protein.

EXPB1 and CW Binding

A total of 1.2 mg of paramagnetic Mn^{2+}-tagged EXPB1 and diamagnetic EXPB1 was incubated for approximately 10 h with 50 mg hydrated CW in

300 μL 20 mM NaOAc buffer, pH 5.5, and 2 mM NaN_3 at 4°C. The water content of the wall-protein mixture was reduced to approximately 75% by centrifugation. The hydrated CW samples were stored frozen prior to SSNMR analysis.

Solid-State NMR Spectroscopy

All SSNMR experiments were measured on a Bruker 900-MHz (21.1 Tesla) spectrometer using a 3.2-mm MAS probe at 296K. Typical radio-frequency strengths were 62.5 to 80 kHz for ^{1}H and 62.5 kHz for ^{13}C. ^{13}C chemical shifts were reported on the tetramethylsilane scale, using the adamantane CH_2 signal at 38.48 ppm as external reference.

1D ^{13}C spectra were measured at 296 K under 13.5-kHz MAS. Initial ^{13}C magnetization was created using either ^{13}C DP or 1 ms ^{1}H-^{13}C CP. Quantitative DP spectra were measured using a recycle delay of 25 s. The difference spectra were obtained by subtracting the spectrum of the paramagnetic sample from that of the diamagnetic sample. A near-unity scaling factor of 0.94 to 1.0 was used to compensate for minor differences in sample amounts. PRE-induced intensity decrease is reported as S/S_0, the ratio of the peak height of the ^{13}C spectrum of the paramagnetic sample with the peak height of the diamagnetic sample. The carbonyl region of the quantitative ^{13}C DP spectra was deconvoluted using Dmfit (Massiot et al., 2002). The full widths at half maximum, the peak heights, and the integrals of the deconvoluted peaks are reported in Supplemental Table S2.

2D ^{1}H-driven ^{13}C spin diffusion (PDSD) spectra were measured at 296 K under 13.5-kHz MAS (Meier, 1994; Bardet et al., 1997). Then 1 ms ^{1}H-^{13}C CP was used to create the initial ^{13}C magnetization. The mixing time was 100 ms to observe intramolecular cross peaks (Wang et al., 2015). All CP-PDSD spectra were measured with 64 scans per t_1 slice, an acquisition time of 14.5 ms in the t_2 dimension, 472 t_1 slices acquired in the states fashion at an increment of 35 μs, which give a maximum t_1 evolution time of 8.3 ms. Difference 2D spectrum was obtained by subtracting the EXPB1-Mn^{2+} spectrum from the EXPB1 spectrum without any scaling factor. All 2D spectra were processed using a QSINE window function with a moderate shifted sine bell of 2.5 and were plotted using Topspin parameters of lev0 = 4.5, Toplev = 40, and nlev = 16.

^{13}C-^{1}H dipolar-chemical shift experiments (Munowitz et al., 1981) were measured under 7-kHz MAS at 296K. ^{1}H homonuclear decoupling was achieved using frequency-switched Lee-Goldburg (Bielecki et al., 1989) with a tilted ^{1}H radio-frequency field strength of 98 kHz. The scaling factor is confirmed to be 0.577 using the model tripeptide formyl-Met-Leu-Phe (Hong and Griffin, 1998; Rienstra et al., 2002). Order parameters were obtained by dividing the measured dipolar couplings by the scaled rigid-limit coupling (13.1 kHz).

Supplemental Data

The following supplemental materials are available.

Supplemental Figure S1. CW extension (creep) activity of heat-inactivated wheat coleoptiles in 50 mM v 20 mM sodium acetate buffer.

Supplemental Figure S2. Dependence of EXPB1 binding to maize silk CW as a function of pH.

Supplemental Figure S3. EXPB1 binding to pure cellulose (Avicel).

Supplemental Figure S4. Characterization of Mn^{2+}-tagged EXPB1.

Supplemental Figure S5. Carbonyl region of the ^{13}C spectra of Arabidopsis, *Brachypodium*, and maize CWs.

Supplemental Figure S6. ^{13}C-^{1}H CP-DIPSHIFT dipolar curves of maize CWs.

Supplemental Table S1. Monosaccharide compositions of CW and extracted polysaccharides after sequential chemical extractions.

Supplemental Table S2. Fitting parameters of the carbonyl signals in ^{13}C quantitative DP spectra.

ACKNOWLEDGMENTS

We thank Ed Wagner and Dr. Tatiana Laremore for technical assistance.

Received August 22, 2016; accepted October 7, 2016; published October 11, 2016.

LITERATURE CITED

Bardet M, Emsley L, Vincendon M (1997) Two-dimensional spin-exchange solid-state NMR studies of ^{13} C-enriched wood. Solid State Nucl Magn Reson **8:** 25–32

Bertini I, Luchinat C, Parigi G (2001) Solution NMR of Paramagnetic Molecules: Applications to Metallobiomolecules and Models. Elsevier, Amsterdam, The Netherlands

Bielecki A, Kolbert AC, Levitt MH (1989) Frequency-switched pulse sequences - homonuclear decoupling and dilute spin NMR in solids. Chem Phys Lett **155:** 341–346

Bloembergen N (1957) Proton relaxation times in paramagnetic solutions. J Chem Phys **27:** 572–573

Bromley JR, Busse-Wicher M, Tryfona T, Mortimer JC, Zhang Z, Brown DM, Dupree P (2013) GUX1 and GUX2 glucuronyltransferases decorate distinct domains of glucuronoxylan with different substitution patterns. Plant J **74:** 423–434

Buanafina MM (2009) Feruloylation in grasses: current and future perspectives. Mol Plant **2:** 861–872

Buffy JJ, Hong T, Yamaguchi S, Waring AJ, Lehrer RI, Hong M (2003) Solid-state NMR investigation of the depth of insertion of protegrin-1 in lipid bilayers using paramagnetic Mn^{2+}. Biophys J **85:** 2363–2373

Busse-Wicher M, Gomes TC, Tryfona T, Nikolovski N, Stott K, Grantham NJ, Bolam DN, Skaf MS, Dupree P (2014) The pattern of xylan acetylation suggests xylan may interact with cellulose microfibrils as a twofold helical screw in the secondary plant cell wall of Arabidopsis thaliana. Plant J **79:** 492–506

Carpita NC (1983) Hemicellulosic polymers of cell walls of zea coleoptiles. Plant Physiol **72:** 515–521

Carpita NC (1996) Structure and biogenesis of the cell walls of grasses. Annu Rev Plant Physiol Plant Mol Biol **47:** 445–476

Carpita NC, Defernez M, Findlay K, Wells B, Shoue DA, Catchpole G, Wilson RH, McCann MC (2001) Cell wall architecture of the elongating maize coleoptile. Plant Physiol **127:** 551–565

Cho HT, Kende H (1997) Expansins in deepwater rice internodes. Plant Physiol **113:** 1137–1143

Cosgrove DJ (2000) Loosening of plant cell walls by expansins. Nature **407:** 321–326

Cosgrove DJ (2011) Measuring in vitro extensibility of growing plant cell walls. Methods Mol Biol **715:** 291–303

Cosgrove DJ (2015) Plant expansins: diversity and interactions with plant cell walls. Curr Opin Plant Biol **25:** 162–172

Cosgrove DJ (2016) Catalysts of plant cell wall loosening. F1000 Res **5:** F1000 Faculty Rev-119.

Cosgrove DJ, Bedinger P, Durachko DM (1997) Group I allergens of grass pollen as cell wall-loosening agents. Proc Natl Acad Sci USA **94:** 6559–6564

Darley CP, Li Y, Schaap P, McQueen-Mason SJ (2003) Expression of a family of expansin-like proteins during the development of *Dictyostelium discoideum*. FEBS Lett **546:** 416–418

Dubois M, Dubois M, Gilles KA, Hamilton JK, Rebers PA, Smith F (1956) Colorimetric method for determination of sugars and related substances. Anal Chem **28:** 350–356

Dupree R, Simmons TJ, Mortimer JC, Patel D, Iuga D, Brown SP, Dupree P (2015) Probing the molecular architecture of *Arabidopsis thaliana* secondary cell walls using two- and three-dimensional (^{13}C solid state nuclear magnetic resonance spectroscopy. Biochemistry **54:** 2335–2345

Ebright YW, Chen Y, Pendergrast PS, Ebright RH (1992) Incorporation of an EDTA-metal complex at a rationally selected site within a protein: application to EDTA-iron DNA affinity cleaving with catabolite gene activator protein (CAP) and Cro. Biochemistry **31:** 10664–10670

Ermácora MR, Delfino JM, Cuenoud B, Schepartz A, Fox RO (1992) Conformation-dependent cleavage of staphylococcal nuclease with a disulfide-linked iron chelate. Proc Natl Acad Sci USA **89:** 6383–6387

Georgelis N, Nikolaidis N, Cosgrove DJ (2014) Biochemical analysis of expansin-like proteins from microbes. Carbohydr Polym **100:** 17–23

Georgelis N, Nikolaidis N, Cosgrove DJ (2015) Bacterial expansins and related proteins from the world of microbes. Appl Microbiol Biotechnol **99:** 3807–3823

Georgelis N, Tabuchi A, Nikolaidis N, Cosgrove DJ (2011) Structure-function analysis of the bacterial expansin EXLX1. J Biol Chem **286:** 16814–16823

Georgelis N, Yennawar NH, Cosgrove DJ (2012) Structural basis for entropy-driven cellulose binding by a type-A cellulose-binding module (CBM) and bacterial expansin. Proc Natl Acad Sci USA **109:** 14830–14835

Gibeaut DM, Pauly M, Bacic A, Fincher GB (2005) Changes in cell wall polysaccharides in developing barley (*Hordeum vulgare*) coleoptiles. Planta **221:** 729–738

Hollmann J, Elbegzaya N, Pawelzik E, Lindhauer MG (2009) Isolation and characterization of glucuronoarabinoxylans from wheat bran obtained by classical and ultrasound-assisted extraction methods. Qual Assur Saf Crop **1:** 231–239

Hong M, Griffin RG (1998) Resonance assignments for solid peptides by dipolar-mediated $^{13}C/^{15}N$ correlation solid-state NMR. J Am Chem Soc **120:** 7113–7114

Ishii S (1984) Cell wall cementing materials of grass leaves. Plant Physiol **76:** 959–961

Jaroniec CP (2015) Structural studies of proteins by paramagnetic solid-state NMR spectroscopy. J Magn Reson **253:** 50–59

Kerff F, Amoroso A, Herman R, Sauvage E, Petrella S, Filée P, Charlier P, Joris B, Tabuchi A, Nikolaidis N, et al (2008) Crystal structure and activity of *Bacillus subtilis* YoaJ (EXLX1), a bacterial expansin that promotes root colonization. Proc Natl Acad Sci USA **105:** 16876–16881

Kern T, Giffard M, Hediger S, Amoroso A, Giustini C, Bui NK, Joris B, Bougault C, Vollmer W, Simorre JP (2010) Dynamics characterization of fully hydrated bacterial cell walls by solid-state NMR: evidence for cooperative binding of metal ions. J Am Chem Soc **132:** 10911–10919

Köhnke T, Ostlund A, Brelid H (2011) Adsorption of arabinoxylan on cellulosic surfaces: influence of degree of substitution and substitution pattern on adsorption characteristics. Biomacromolecules **12:** 2633–2641

Kubicki JD, Mohamed MNA, Watts HD (2013) Quantum mechanical modeling of the structures, energetics and spectral properties of I alpha and I beta cellulose. Cellulose **20:** 9–23

Kubicki JD, Watts HD, Zhao Z, Zhong LH (2014) Quantum mechanical calculations on cellulose-water interactions: structures, energetics, vibrational frequencies and NMR chemical shifts for surfaces of I alpha and I beta cellulose. Cellulose **21:** 909–926

Li LC, Bedinger PA, Volk C, Jones AD, Cosgrove DJ (2003) Purification and characterization of four beta-expansins (Zea m 1 isoforms) from maize pollen. Plant Physiol **132:** 2073–2085

Li Y, Darley CP, Ongaro V, Fleming A, Schipper O, Baldauf SL, McQueen-Mason SJ (2002) Plant expansins are a complex multigene family with an ancient evolutionary origin. Plant Physiol **128:** 854–864

Maltsev S, Hudson SM, Sahu ID, Liu L, Lorigan GA (2014) Solid-state NMR (^{31}P paramagnetic relaxation enhancement membrane protein immersion depth measurements. J Phys Chem B **118:** 4370–4377

Marbella LE, Cho HS, Spence MM (2013) Observing the translocation of a mitochondria-penetrating peptide with solid-state NMR. Biochim Biophys Acta **1828:** 1674–1682

Massiot D, Fayon F, Capron M, King I, Le Calve S, Alonso B, Durand JO, Bujoli B, Gan ZH, Hoatson G (2002) Modelling one- and two-dimensional solid-state NMR spectra. Magn Reson Chem **40:** 70–76

McQueen-Mason S, Durachko DM, Cosgrove DJ (1992) Two endogenous proteins that induce cell wall extension in plants. Plant Cell **4:** 1425–1433

McQueen-Mason SJ, Cosgrove DJ (1995) Expansin mode of action on cell walls. Analysis of wall hydrolysis, stress relaxation, and binding. Plant Physiol **107:** 87–100

Meier BH (1994) Polarization transfer and spin diffusion in solid-state NMR. Adv Magn Opt Reson **18:** 1–116

Munowitz MG, Griffin RG, Bodenhausen G, Huang TH (1981) Two-dimensional rotational spin-echo nuclear magnetic-resonance in solids: correlation of chemical-shift and dipolar interactions. J Am Chem Soc **103:** 2529–2533

Nadaud PS, Helmus JJ, Kall SL, Jaroniec CP (2009) Paramagnetic ions enable tuning of nuclear relaxation rates and provide long-range structural restraints in solid-state NMR of proteins. J Am Chem Soc **131:** 8108–8120

Nikolaidis N, Doran N, Cosgrove DJ (2014) Plant expansins in bacteria and fungi: evolution by horizontal gene transfer and independent domain fusion. Mol Biol Evol **31:** 376–386

Rienstra CM, Tucker-Kellogg L, Jaroniec CP, Hohwy M, Reif B, McMahon MT, Tidor B, Lozano-Pérez T, Griffin RG (2002) De novo determination of peptide structure with solid-state magic-angle spinning NMR spectroscopy. Proc Natl Acad Sci USA **99:** 10260–10265

Sampedro J, Cosgrove DJ (2005) The expansin superfamily. Genome Biol **6:** 242

Sampedro J, Guttman M, Li LC, Cosgrove DJ (2015) Evolutionary divergence of β-expansin structure and function in grasses parallels emergence of distinctive primary cell wall traits. Plant J **81:** 108–120

Selig MJ, Thygesen LG, Felby C, Master ER (2015) Debranching of soluble wheat arabinoxylan dramatically enhances recalcitrant binding to cellulose. Biotechnol Lett **37:** 633–641

Sengupta I, Gao M, Arachchige RJ, Nadaud PS, Cunningham TF, Saxena S, Schwieters CD, Jaroniec CP (2015) Protein structural studies by paramagnetic solid-state NMR spectroscopy aided by a compact cyclen-type Cu(II) binding tag. J Biomol NMR **61:** 1–6

Sengupta I, Nadaud PS, Helmus JJ, Schwieters CD, Jaroniec CP (2012) Protein fold determined by paramagnetic magic-angle spinning solid-state NMR spectroscopy. Nat Chem **4:** 410–417

Solomon I (1955) Relaxation processes in a system of two spins. Phys Rev **99:** 559–565

Su Y, Hu F, Hong M (2012) Paramagnetic Cu(II) for probing membrane protein structure and function: inhibition mechanism of the influenza M2 proton channel. J Am Chem Soc **134:** 8693–8702

Tabuchi A, Li LC, Cosgrove DJ (2011) Matrix solubilization and cell wall weakening by β-expansin (group-1 allergen) from maize pollen. Plant J **68:** 546–559

Valdivia ER, Stephenson AG, Durachko DM, Cosgrove D (2009) Class B beta-expansins are needed for pollen separation and stigma penetration. Sex Plant Reprod **22:** 141–152

Valdivia ER, Wu Y, Li LC, Cosgrove DJ, Stephenson AG (2007) A group-1 grass pollen allergen influences the outcome of pollen competition in maize. PLoS One **2:** e154

Viëtor RJ, Newman RH, Ha MA, Apperley DC, Jarvis MC (2002) Conformational features of crystal-surface cellulose from higher plants. Plant J **30:** 721–731

Vignon MR, Gey C (1998) Isolation, ^{1}H and ^{13}C NMR studies of (4-O-methyl-D-glucurono)-D-xylans from luffa fruit fibres, jute bast fibres and mucilage of quince tree seeds. Carbohydr Res **307:** 107–111

Vogel J (2008) Unique aspects of the grass cell wall. Curr Opin Plant Biol **11:** 301–307

Wang T, Hong M (2016) Solid-state NMR investigations of cellulose structure and interactions with matrix polysaccharides in plant primary cell walls. J Exp Bot **67:** 503–514

Wang T, Park YB, Caporini MA, Rosay M, Zhong L, Cosgrove DJ, Hong M (2013) Sensitivity-enhanced solid-state NMR detection of expansin's target in plant cell walls. Proc Natl Acad Sci USA **110:** 16444–16449

Wang T, Salazar A, Zabotina OA, Hong M (2014) Structure and dynamics of *Brachypodium* primary cell wall polysaccharides from two-dimensional ^{13}C solid-state nuclear magnetic resonance spectroscopy. Biochemistry **53:** 2840–2854

Wang T, Williams JK, Schmidt-Rohr K, Hong M (2015) Relaxation-compensated difference spin diffusion NMR for detecting 13C-13C long-range correlations in proteins and polysaccharides. J Biomol NMR **61:** 97–107

Wang T, Yang H, Kubicki JD, Hong M (2016) Cellulose structural polymorphism in plant primary cell walls investigated by high-field 2D solid-state NMR spectroscopy and density functional theory calculations. Biomacromolecules **17:** 2210–2222

Wang T, Zabotina O, Hong M (2012) Pectin-cellulose interactions in the Arabidopsis primary cell wall from two-dimensional magic-angle-spinning solid-state nuclear magnetic resonance. Biochemistry **51:** 9846–9856

Watts HD, Mohamed MNA, Kubicki JD (2013) A DFT study of vibrational frequencies and ^{13}C NMR chemical shifts of model cellulosic fragments as a function of size. Cellulose **21:** 53–70

White PB, Wang T, Park YB, Cosgrove DJ, Hong M (2014) Water-polysaccharide interactions in the primary cell wall of *Arabidopsis thaliana* from polarization transfer solid-state NMR. J Am Chem Soc **136:** 10399–10409

Yennawar NH, Li LC, Dudzinski DM, Tabuchi A, Cosgrove DJ (2006) Crystal structure and activities of EXPB1 (Zea m 1), a beta-expansin and group-1 pollen allergen from maize. Proc Natl Acad Sci USA **103:** 14664–14671

Yuan S, Wu Y, Cosgrove DJ (2001) A fungal endoglucanase with plant cell wall extension activity. Plant Physiol **127:** 324–333

Zhao Z, Crespi VH, Kubicki JD, Cosgrove DJ, Zhong LH (2014) Molecular dynamics simulation study of xyloglucan adsorption on cellulose surfaces: effects of surface hydrophobicity and side-chain variation. Cellulose **21:** 1025–1039